

Behavior of Atomic and Molecular Hydrogen by Using the Measurements of H_{α} Line Emission in the GAMMA 10 Tandem Mirror

KUBOTA Yuusuke, YOSHIKAWA Masayuki, NAKASHIMA Yousuke, SAWADA Keiji¹, KOBAYASHI Takayuki, SAITO Masashi, HIGASHIZONO Yuta, ITAKURA Akiyosi and CHO Teruji

Plasma Research Center, University of Tsukuba, Tsukuba 305-8577, Japan

¹*Faculty of Engineering, Shinshu University, Nagano 380-8553, Japan*

(Received: 4 October 2004 / Accepted: 24 May 2005)

Abstract

The effective rate coefficients for atomic and molecular hydrogen are calculated based on collisional-radiative model and the rate coefficients of several atomic and molecular processes. The results indicate that the effect of atomic hydrogen is dominant for H_{α} line emission and the effect of molecular hydrogen for the ionization rate is larger than that of atomic hydrogen at the parameter range of the GAMMA 10 central cell. Moreover the atomic and molecular hydrogen densities are estimated by H_{α} line emission. From the evaluation of the ionization rate by using the estimated neutral hydrogen densities, it is necessary to consider the behavior of molecular hydrogen for analysis of the particle balance in GAMMA 10.

Keywords:

neutral hydrogen, ionization rate, H_{α} line emission, particle balance, GAMMA 10

1. Introduction

In magnetically confined plasmas, a neutral hydrogen behavior is an important subject to clarify the particle balance. Measurements of H_{α} line emission from the plasmas are also important to evaluate particle and energy confinement. In the GAMMA 10 tandem mirror, the ionization rate is estimated experimentally by the measurements of an electron density and H_{α} line emission. The ionization rate and H_{α} line emission depend on the atomic hydrogen and molecular hydrogen. However it is difficult to separate the contributions from the atomic hydrogen and the molecular hydrogen on the measurement of H_{α} line emission. Then we calculated an effective rate coefficient of atomic and molecular hydrogen for H_{α} line emission by using collisional-radiative model (CR-model) [1] and evaluated an ionization rate based on the rate coefficients of several atomic and molecular processes. From these calculation results and the measurements of H_{α} line emission, atomic and molecular hydrogen densities and the ionization rate in the mid-plane of the GAMMA 10 central cell are estimated. In this article, we show the calculation results of the effects of atomic and molecular hydrogen and discuss the particle balance near the mid-plane of the central cell.

2. Experimental apparatuses

GAMMA 10 is a 27 m long tandem mirror plasma

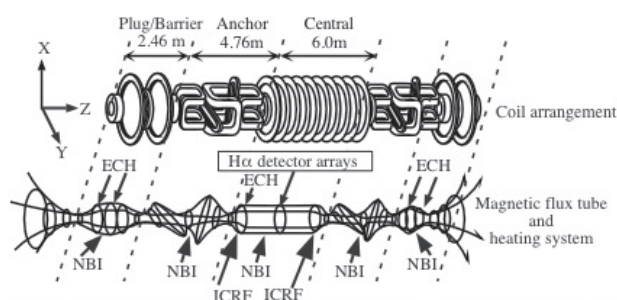


Fig. 1 The schematic view of the GAMMA 10 tandem mirror.

confinement device with a thermal barrier. It consists of a 5.6 m long axisymmetric central cell, two anchor cells for suppressing magnetohydrodynamic (MHD) instabilities which are located in both ends of the central cell. Two plug/barrier cells are connected to the anchor cells for forming the plug and thermal barrier potentials. Figure 1 shows the schematic view of the GAMMA 10 tandem mirror. In the GAMMA 10 plasma, the confinement is achieved by not only a magnetic mirror configuration but also high potentials at the both plug/barrier cells. The potentials are produced by means of the electron cyclotron resonance heating (ECRH) at the plug/barrier cells. The main plasma is produced and heated by the ion cyclotron range of frequency (ICRF) waves. In plasmas produced in the core region of the

central cell, typical electron density, electron temperature and ion temperature are about $2 \times 10^{12} \text{ cm}^{-3}$, 100 eV and 5 keV, respectively.

The line-integrated electron density of the plasma is measured with the microwave interferometer. The interferometer mounted on the mid-plane of the central cell can be scanned along the Y-axis of GAMMA 10. The radial profile of electron density is obtained by using the Abel inversion.

H_α line emissions are measured with detectors which consist of H_α interference filters, focusing lenses, apertures, optical fibers and photomultiplier tubes (PMTs). Near the mid-plane of the central cell, vertical and horizontal arrays of H_α detectors are installed to measure the spatial profiles of H_α brightness [2,3]. Each array has 12 channel detectors. The output signals from the PMTs are amplified and led to a CAMAC system. This system is absolutely calibrated by a standard lamp. From the measurement results of these arrays, the spatial profile of H_α emissivity is obtained by using Algebraic Reconstruction Technique (ART) [4].

3. Calculation results

3.1 Effective rate coefficient for H_α line emission

H_α emissivity is shown as below.

$$E(H_\alpha) = \frac{\epsilon_{H_\alpha} A_{32}}{4\pi} n(3), \quad (1)$$

where A_{32} , ϵ_{H_α} , $n(3)$ are the transition probability of H_α , the energy of H_α line emission and the population density of $n = 3$ of hydrogen atoms, respectively. Moreover $n(3)$ is shown as

$$n(3) = n_e n_H R_1(3) + n_e n_{H_2} R_2(3), \quad (2)$$

where n_e , n_H , n_{H_2} , $R_1(3)$, $R_2(3)$ are the electron density, the atomic hydrogen density, the molecular hydrogen density, the effective rate coefficient of atomic hydrogen, the effective rate coefficient of molecular hydrogen, respectively. $R_1(3)$ and $R_2(3)$ can be obtained by using CR-model. $R_1(3)$ and $R_2(3)$ indicate the effect of atomic and molecular hydrogen for H_α emissivity. The calculation results of $R_1(3)$ and $R_2(3)$ are shown in Fig. 2. In Fig. 2, it is found that $R_2(3)$ that originates a dissociative-excitation is about one tenth on the $R_1(3)$ at the plasma parameter of the GAMMA 10 central cell. In the central cell, electron density and electron temperature are $3 \times 10^{12} \text{ cm}^{-3}$ (core region) $-5 \times 10^{11} \text{ cm}^{-3}$ (peripheral region), 100 eV (core) -20 eV (peripheral) in this case without ECRH, respectively. For H_α line emission, the effect of atomic hydrogen is dominant to that of molecular hydrogen.

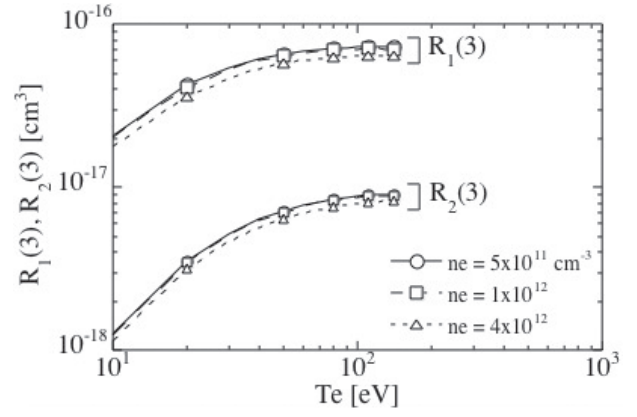
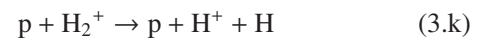
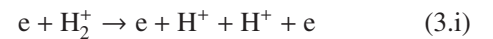
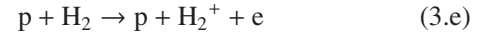
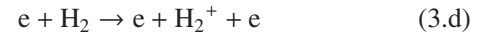
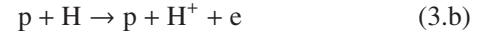


Fig. 2 The calculation results of $R_1(3)$ and $R_2(3)$ by using CR-model.

3.2 Effective rate coefficients for the ionization rate

The ionization rate is determined by atom-electron, atom-ion, molecule-electron and molecule-ion collisions. These collisions include several reactions, which are ionization, ionization of molecule, dissociation, etc. [5,6]. Considered processes are shown below.



The ionization rate equation is shown as follows,

$$\begin{aligned} s &= n_e n_H \langle \sigma v \rangle_e^H + n_i n_H \langle \sigma v \rangle_p^H \\ &\quad + n_e n_{H_2} \langle \sigma v \rangle_e^{H_2} + n_i n_{H_2} \langle \sigma v \rangle_p^{H_2} \\ &= n_e n_H [\langle \sigma v \rangle_e^H + \langle \sigma v \rangle_p^H] + n_e n_{H_2} [\langle \sigma v \rangle_e^{H_2} + \langle \sigma v \rangle_p^{H_2}] \\ &= n_e n_H \langle \sigma v \rangle_{total}^H + n_e n_{H_2} \langle \sigma v \rangle_{total}^{H_2}, \end{aligned} \quad (4)$$

where the subscript e and p represent electron and proton, respectively. The effective rate coefficients in Eq. 4 can be rewritten as follows by using the rate coefficients of the reactions 3.a-3.k [5].

$$\langle \sigma v \rangle_e^H = \langle \sigma v \rangle_{3.a}$$

$$\langle \sigma v \rangle_p^H = \langle \sigma v \rangle_{3.b}$$

$$\langle \sigma v \rangle_e^{H_2} = \langle \sigma v \rangle_{3.c} + \eta \langle \sigma v \rangle_{3.d}$$

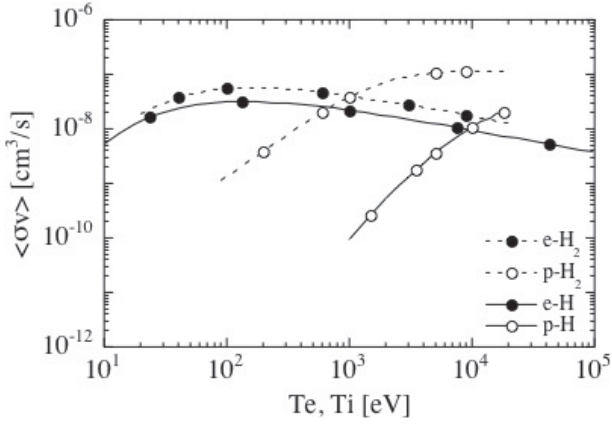


Fig. 3 The effective rate coefficients for the ionization. ex. e-H : electron - atomic hydrogen collision.

$$\langle\sigma v\rangle_p^{H_2} = \eta(\langle\sigma v\rangle_{3,e} + \langle\sigma v\rangle_{3,f})$$

$$\eta = \frac{\langle\sigma v\rangle_{3,h} + 2\langle\sigma v\rangle_{3,i} + \langle\sigma v\rangle_{3,j} + \langle\sigma v\rangle_{3,k}}{\langle\sigma v\rangle_{3,g} + \langle\sigma v\rangle_{3,h} + \langle\sigma v\rangle_{3,i} + \langle\sigma v\rangle_{3,j} + \langle\sigma v\rangle_{3,k}} \quad (5)$$

The calculation results of rate coefficients are shown in Fig. 3. In figure, it is found that the effect of molecular hydrogen for the ionization rate is several times larger than that of atomic hydrogen at the parameter range of the central cell. The ion temperature is 6 keV (core) – 500 eV (peripheral) in the central cell. In particular, the contribution from molecular hydrogen for ionization rate is dominant in the peripheral region, because both density and rate coefficient of molecular hydrogen are larger than those of atomic hydrogen.

4. Experimental results and discussion

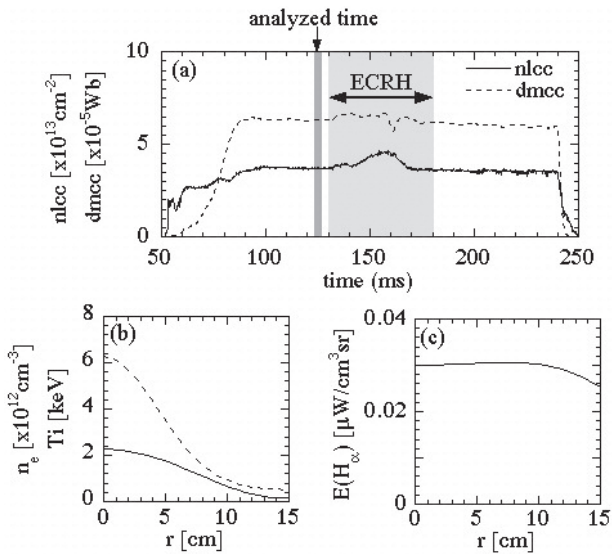


Fig. 4 Temporal behavior of line-integrated electron density and the diamagnetism (a), the radial profiles of electron density and ion temperature (b) and the profile of H_α emissivity (c) at 125 ms.

Temporal behavior of line-integrated electron density and the diamagnetism (a), the radial profiles of electron density and ion temperature (b) and the profile of H_α emissivity (c) at 125 ms are shown in Fig. 4. The typical electron temperature profile [7] is used for calculation. The plasma of this experiment is ICRF-heated plasma with ECRH (130 ms to 180 ms). The plasma is heated only ICRF-heating at the analyzed time of 125 ms.

4.1 Estimation of the radial profiles of atomic and molecular hydrogen

As the preparation for the estimation of the radial profiles, n_H^{max} and $n_{H_2}^{max}$ are defined as below,

$$n_H^{max} \equiv \frac{E(H_\alpha)}{\alpha n_e R_1(3)}, \quad n_{H_2}^{max} \equiv \frac{E(H_\alpha)}{\alpha n_e R_2(3)}$$

$$\alpha = \frac{\epsilon_{H_\alpha} A_{32}}{4\pi} \quad (6)$$

The n_H^{max} and $n_{H_2}^{max}$ indicate maximum density of atomic and molecular hydrogen obtained by the H_α emissivity. From eq. 1, eq. 2 and eq. 6, the relationship between n_H , n_{H_2} and $n_{H_2}^{max}$ is expressed as

$$n_{H_2}^{max} = \frac{R_1(3)}{R_2(3)} n_H + n_{H_2}. \quad (7)$$

Because the radial profile of n_H is flat compared with that of n_{H_2} [8] and the profile of $R_1(3)/R_2(3)$ is also flat, it is supposed that the profile shape of $n_{H_2}^{max}$ is determined by that of n_{H_2} . Assuming that no molecular hydrogen exist in the center of the plasma, $n_H(r=0)$ is equal to $n_H^{max}(r=0)$. Then $n_H^{max}(r=0)$ is substituted for n_H in eq. 7, n_{H_2} is shown as

$$n_{H_2}(r) = C \left(n_{H_2}^{max}(r) - \frac{R_1(3)}{R_2(3)}(r) n_H^{max}(r=0) \right), \quad (8)$$

where C is a constant to evaluate the absolute value of

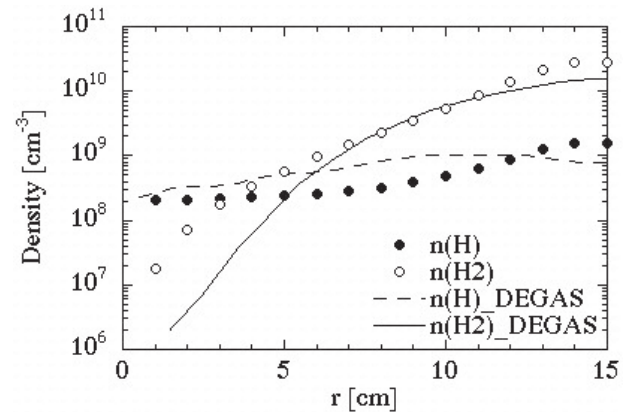


Fig. 5 The radial profiles of atomic and molecular hydrogen estimated by the new method and those obtained by DEGAS code.

n_{H_2} . It is assumed to determine the C that all neutral hydrogen is molecular hydrogen in the boundary of the plasma ($r = 20$ cm). However, there is no data at $r = 20$ cm. Then assuming again that $n_{H_2}(r = 10$ cm) is equal to the half of $n_{H_2}^{max}(r = 10$ cm), C is determined as

$$C = \frac{0.5n_{H_2}^{max}(r = 10)}{n_{H_2}^{max}(r = 10) - \frac{R_1(3)}{R_2(3)}(r = 10)n_{H_2}^{max}(r = 0)} \quad (9)$$

Therefore $n_{H_2}(r)$ is obtained. $n_H(r)$ is also obtained from eq. 7 as below,

$$n_H(r) = \frac{R_2(3)}{R_1(3)}(n_{H_2}^{max}(r) - n_{H_2}(r)). \quad (10)$$

The radial profiles of atomic and molecular hydrogen estimated by the above method and those obtained by DEGAS simulation code [9] in which the molecular-dissociation effects are taken into account [10] are shown in Fig. 5. From the figure, the profiles estimated by the above method almost agree with those obtained by DEGAS code. Therefore the rough estimation of the radial profiles of atomic and molecular hydrogen can be obtained by the above method. However, the above method has some points of notice. First, the molecular hydrogen density estimated by the above method is larger than the results of DEGAS code in the core region. Next, the above method has very weak sensibility to the electron temperature and no sensibility to the ion temperature because $R_1(3)$ and $R_2(3)$ only have weak sensibility to the electron temperature in the central cell parameter range.

4.2 The contributions from atomic and molecular hydrogen for ionization rate

The ionization rate (s [$1/\text{cm}^3\text{s}$]) is obtained by using n_H and n_{H_2} estimated in last section and Eq. 3. The ionization rate s , the ionization rate from atomic hydrogen $s^H = n_e n_H \langle \sigma v \rangle_{total}^H$ and the ionization rate from molecular hydrogen $s^{H_2} = n_e n_{H_2} \langle \sigma v \rangle_{total}^{H_2}$ are shown in Fig. 6.

From Fig. 6, it is found that s is nearly equal to s^{H_2} excluding core region. In particular, s^{H_2} is about one hundred times larger than s^H in the peripheral region. The contribution from molecular hydrogen for ionization rate is dominant to that of atomic hydrogen. The total ionization rate near the mid-plane of the central cell is determined by the ionization rate from molecular hydrogen in this experiment.

5. Summary

We calculated the effective rate coefficients for H_{α} line emission and the ionization rate. The calculation results indicate that the effect of atomic hydrogen is dominant for H_{α} line emission and the effect of

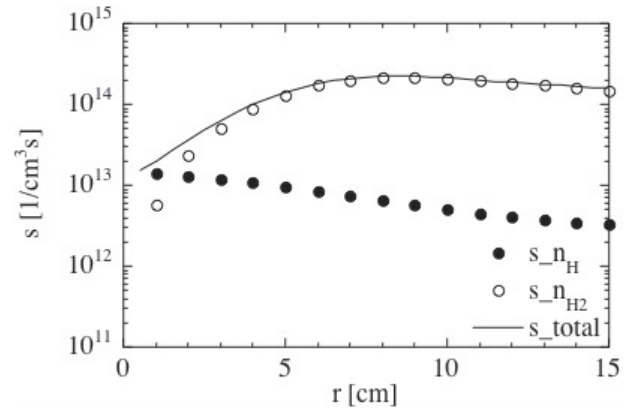


Fig. 6 The radial profiles of the total ionization rate s and the ionization rate from atomic and molecular hydrogen s^H and s^{H_2} .

molecular hydrogen for the ionization rate is larger than that of atomic hydrogen in the central cell parameter range. Moreover, we estimated the radial profiles of atomic and molecular hydrogen densities based on the measured results of H_{α} line emission together with the above-obtained effective rate coefficients. Those profiles almost agree with the profiles obtained by DEGAS code. As the result of the evaluation of the ionization rate based on the estimated neutral hydrogen density profiles, the contribution from molecular hydrogen have a dominant role in the ionization rate near the mid-plane of the central cell. Therefore it is necessary to consider the behavior of molecular hydrogen for analysis of the particle balance of GAMMA 10.

Acknowledgements

The authors would like to thank members of the GAMMA 10 group of the University of Tsukuba.

References

- [1] K. Sawada *et al.*, Phys. Rev. E **49**, 5565 (1994).
- [2] M. Yoshikawa *et al.*, Trans. Fusion Technol. **35**, 273 (1999).
- [3] Y. Kubota *et al.*, to be printed in J. Plasma Fusion Res. SERIES **6** (2004).
- [4] A. Macovski, *Medical Imaging Systems* (PRENTICE-HALL, INC.).
- [5] S. Kobayashi, Ph. D. Thesis Tsukuba Univ. (2001).
- [6] R.K. Janev, W.D. Langer, K. Evans, Jr. and D. E. Post, Jr., *Elementary Processes in Hydrogen-Helium Plasmas* (Springer-Verlag, Berlin, 1987).
- [7] R. Minami *et al.*, Plasma Phys. Control. Fusion **44**, 1363 (2002).
- [8] Y. Nakashima *et al.*, J. Nucl. Mater. **313-316**, 553 (2003).

- [9] D. Heifetz, D. Post, M. Petravac *et al.*, *J. Comput. Phys.* **46**, 309 (1982).
- [10] Y. Nakashima *et al.*, *J. Nucl. Mater.* **196-198**, 493 (1992).